

SUPPLEMENTAL MATERIAL

Hemodynamic Correlates of Blood Pressure Across the Adult Age Spectrum: Noninvasive Evaluation in the Framingham Heart Study

Gary F. Mitchell, MD,¹ Na Wang, MA,² Joseph N. Palmisano, MPH,²
Martin G. Larson, ScD,^{3,4} Naomi M. Hamburg, MD,^{6,7}
Joseph A. Vita, MD,^{6,7} Daniel Levy, MD,^{4,5}
Emelia J. Benjamin, MD, ScM^{4,6,7,8*} and Ramachandran S. Vasan, MD,^{4,6,7,8*}

¹Cardiovascular Engineering, Inc., Norwood, MA; ²Data Coordinating Center, Boston University School of Public Health, Boston, MA; ³Department of Mathematics and Statistics, Boston University, Boston, MA; ⁴NHLBI's Framingham Study, Framingham, MA; ⁵National Heart, Lung, and Blood Institute, Bethesda, MD; ⁶Evans Department of Medicine, ⁷Whitaker Cardiovascular Institute, and ⁸Preventive Medicine and Cardiology Sections, Boston University School of Medicine, Boston, MA; *These authors contributed equally to this work.

Address correspondence to:
Gary F. Mitchell, MD
Cardiovascular Engineering, Inc.
1 Edgewater Drive, Suite 201A
Norwood, MA 02062
Phone: (781) 255-6930
Fax: (781) 255-6931
Email: GaryFMitchell@mindspring.com

Supplemental Methods

Noninvasive hemodynamic data acquisition. Participants were studied in the supine position after resting for approximately 5 minutes. Auscultatory blood pressure was assessed at the level of the brachial artery by using a computer-controlled device that automatically inflated the cuff to a user preset maximum pressure (160 mm Hg) and then precisely controlled deflation at 2 mm Hg/sec. If Korotkoff sounds were detected immediately after cuff inflation, the acquisition was aborted and repeated with maximum cuff pressure increased by 40 mm Hg, up to a maximum of 240 mm Hg. The device digitized and recorded mean cuff pressure and a cuff microphone channel (12 kHz) throughout the inflation and deflation sequence so that auscultatory blood pressure measurements could be over-read by the core laboratory (Cardiovascular Engineering, Inc., Norwood, MA) by analysts who were blinded to participant characteristics. Arterial tonometry with electrocardiogram was obtained from the brachial, radial, femoral and carotid arteries using a custom transducer (Cardiovascular Engineering, Inc., Norwood, MA). Next, 2-dimensional echocardiographic images of the left ventricular outflow tract were obtained from a parasternal long axis view followed by pulsed Doppler of the left ventricular outflow tract from an apical 5-chamber view. Body surface measurements from suprasternal notch to pulse recording sites were obtained by using a fiberglass tape measure for carotid, brachial and radial sites and a caliper for the femoral site.

Tonometric measurements. Tonometry waveforms were signal-averaged using the electrocardiographic R-wave as a fiducial point. Average systolic and diastolic cuff pressures were used to calibrate peak and trough of the signal-averaged brachial waveform. Diastolic and integrated mean brachial pressures were then used to

calibrate carotid waveforms.¹ Carotid-femoral (CFPWV) and carotid-brachial (CBPWV) pulse wave velocities were calculated as described previously.² Reflected wave transit time and augmentation index (AI) were assessed from the carotid pressure waveform (**Figure S1**).³ Left ventricular outflow tract diameter was measured by finding the largest early systolic diameter at a point just proximal to the aortic leaflets. The left ventricular outflow tract Doppler flow velocity waveform was multiplied by outflow tract area to compute aortic volume flow. Cardiac output was defined as the integrated mean of the signal-averaged volume flow waveform. Peripheral resistance was computed by dividing mean arterial pressure by cardiac output. Characteristic impedance of the aorta (Z_c) was computed in the time domain by dividing the increase in pressure during early systole by the corresponding increase in volume flow.⁴ Forward and reflected pressure waves were separated and the amplitude (peak minus trough) of each wave was assessed.⁵ The global reflection factor was computed as reflected wave amplitude divided by forward wave amplitude. Reflected wave overlap with systole was computed by expressing the difference between systolic ejection period and reflected wave transit time as a fraction of systolic ejection period. Apparent pressure amplification was computed as the percentage difference between carotid and brachial pulse pressure (**Figure S2**). True amplification was computed as the percentage difference between central forward wave amplitude and brachial pulse pressure. Total arterial compliance was assessed during the latter two-thirds of diastole using the area method.⁶

Supplemental Table S1. Estimates of age slopes before and after 50 years of age and the difference in slope (older minus younger).

Variables	<50 years*	≥50 years*	Difference*
Blood pressure, mm Hg			
Systolic	3.4±0.3	10.2±0.2	6.8±0.5
Diastolic	4.3±0.2	-1.8±0.1	-6.2±0.3
Mean	4.8±0.2	2.3±0.2	-2.5±0.3
Brachial pulse pressure	-0.9±0.2	12.0±0.2	12.9±0.4
Central pulse pressure	1.2±0.3	12.0±0.2	10.9±0.5
Characteristic impedance, dyne x sec/cm⁵	-8.4±1.3	51.1±1.1	59.5±2.0
Carotid-femoral pulse wave velocity, m/s	0.52±0.04	2.05±0.03	1.53±0.07
Carotid-brachial pulse wave velocity, m/s	0.65±0.03	0.14±0.03	-0.51±0.05
Augmentation index, %	7.6±0.2	-1.6±0.2	-9.2±0.4
Reflected wave transit time, ms	-11.0±0.5	4.9±0.4	15.9±0.8
Reflection factor, ratio	0.023±0.001	-0.004±0.001	-0.027±0.002

*Slopes are expressed per decade of age. All values shown are $P<0.001$.

Supplemental Figure Legends

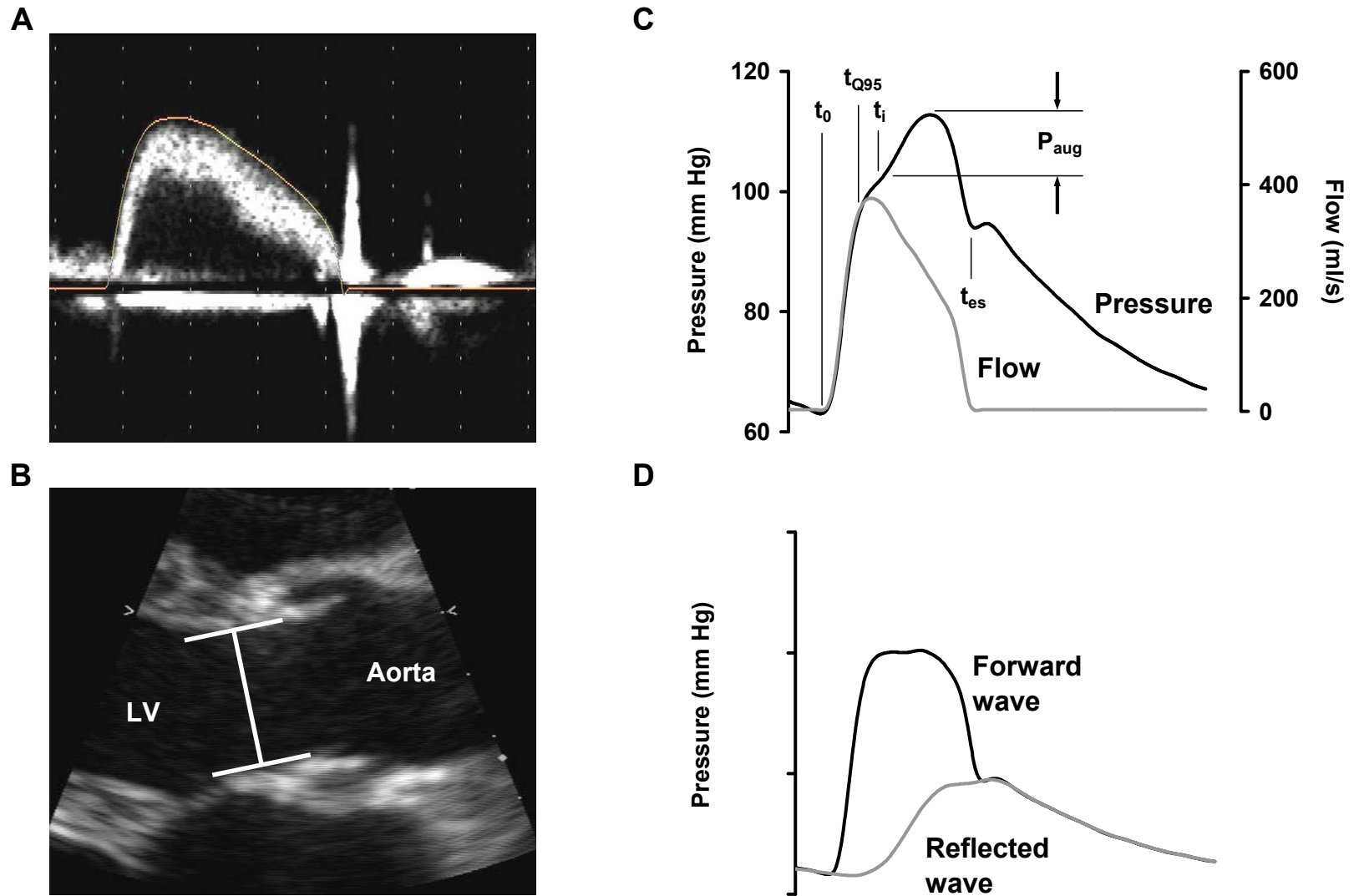
Figure S1. Central pressure-flow analysis. A. Left ventricular outflow tract Doppler flow velocity is obtained from the leading edge of the signal averaged flow spectrum. B. To convert flow velocity to volume flow, the waveform is multiplied by left ventricular outflow tract area, which is computed from measured diameter by assuming a circular cross section. C. The resulting volume flow waveform is paired with carotid tonometry pressure by aligning the foot (t_0) of the respective signal averaged waveforms. The point at which flow reaches 95% of its peak (t_{Q95}) is identified. The corresponding pressure change between t_0 and t_{Q95} is determined. Characteristic impedance is the ratio of change in pressure to change in flow in the window between t_0 to t_{Q95} . Flow has been shifted to the pressure foot and rescaled by characteristic impedance to illustrate the direct correspondence between pressure and flow during this time interval, prior to arrival of the reflected wave. Augmentation index is computed by identifying an inflection point (t_i) in the central pressure waveform and expressing the change in pressure from t_i to peak pressure as a percentage of central pulse pressure. If t_i occurs after peak pressure, augmentation is negative. Note that the computation of characteristic impedance is not dependent on the location of t_i . Temporal overlap between the reflected wave and systolic ejection (t_{es}) was computed as $(t_{es} - t_i)/t_{es}$ D. When pressure and flow are both known, the pressure waveform can be separated into forward and reflected waves. The ratio of reflected to forward wave amplitude is the global reflection factor.

Figure S2. Pressure waveform amplification. True amplification quantifies the percentage difference between central forward pressure wave amplitude and peripheral pulse pressure. Apparent amplification quantifies the percentage difference in overall pulse pressure between central and peripheral sites. Note that augmentation of the central pressure waveform by a reflected pressure wave obscures true amplification, resulting in diminished apparent amplification.

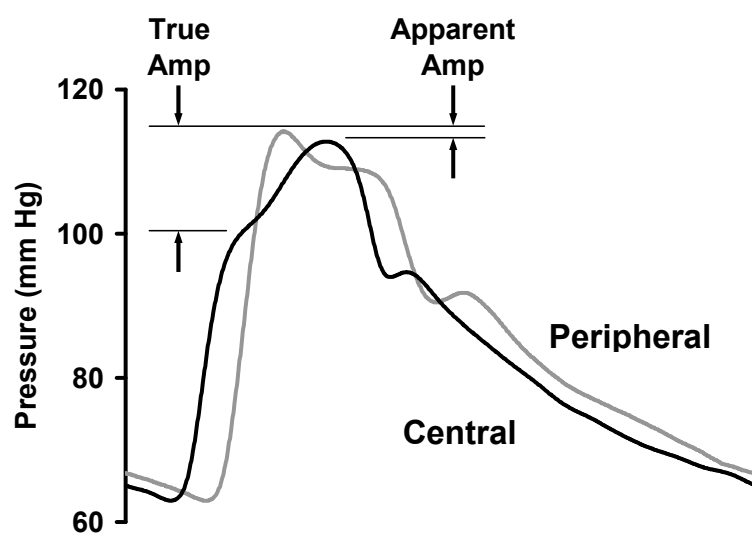
Figure S3. Key hemodynamic variables summarized separately by sex and decades of age. All abbreviations are as per Figure 1.

Figure S4. Pressure amplification and measures of wave reflection summarized separately by sex and decades of age. All abbreviations are as per Figure 2.

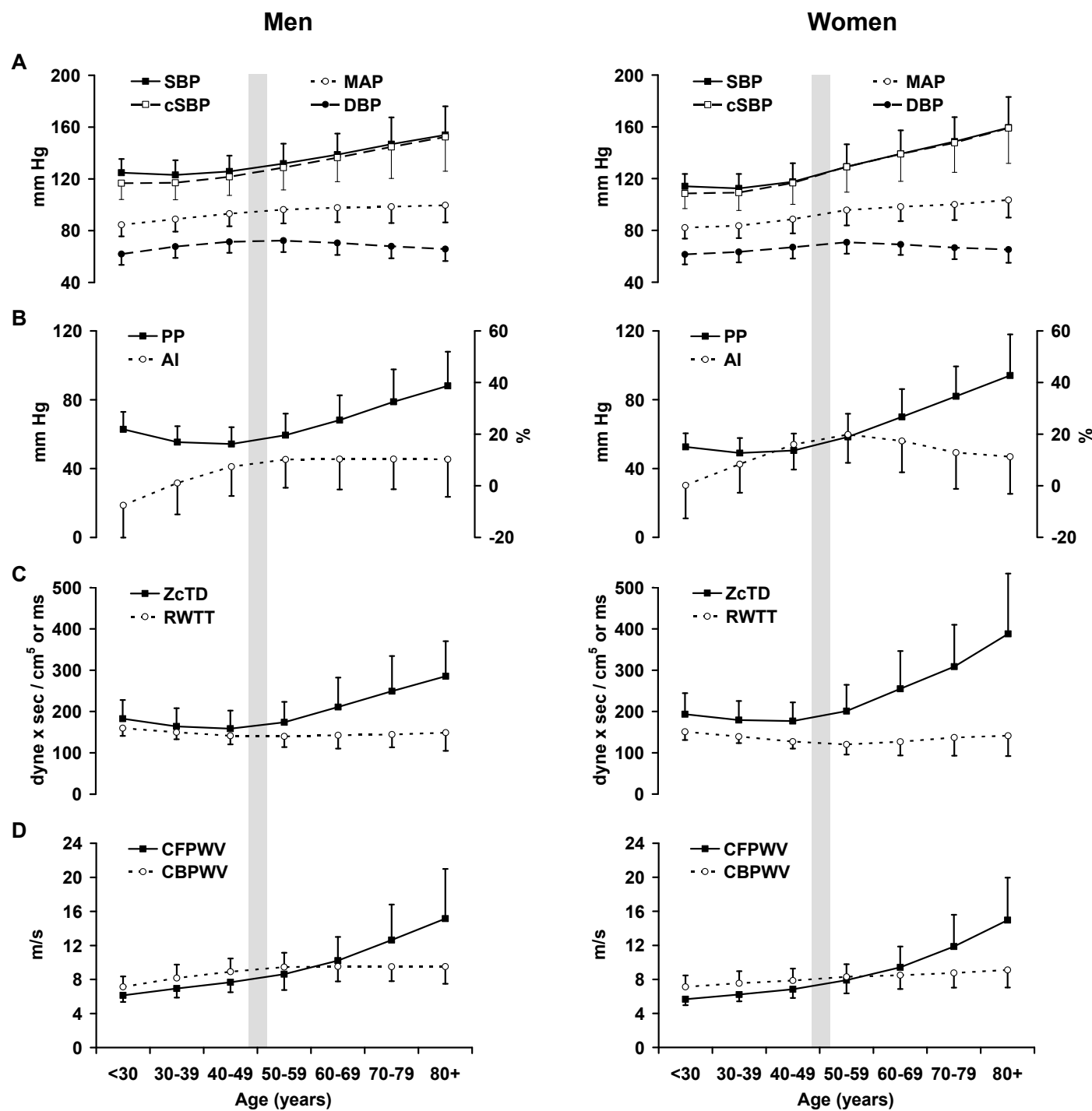
Supplemental Figure S1.



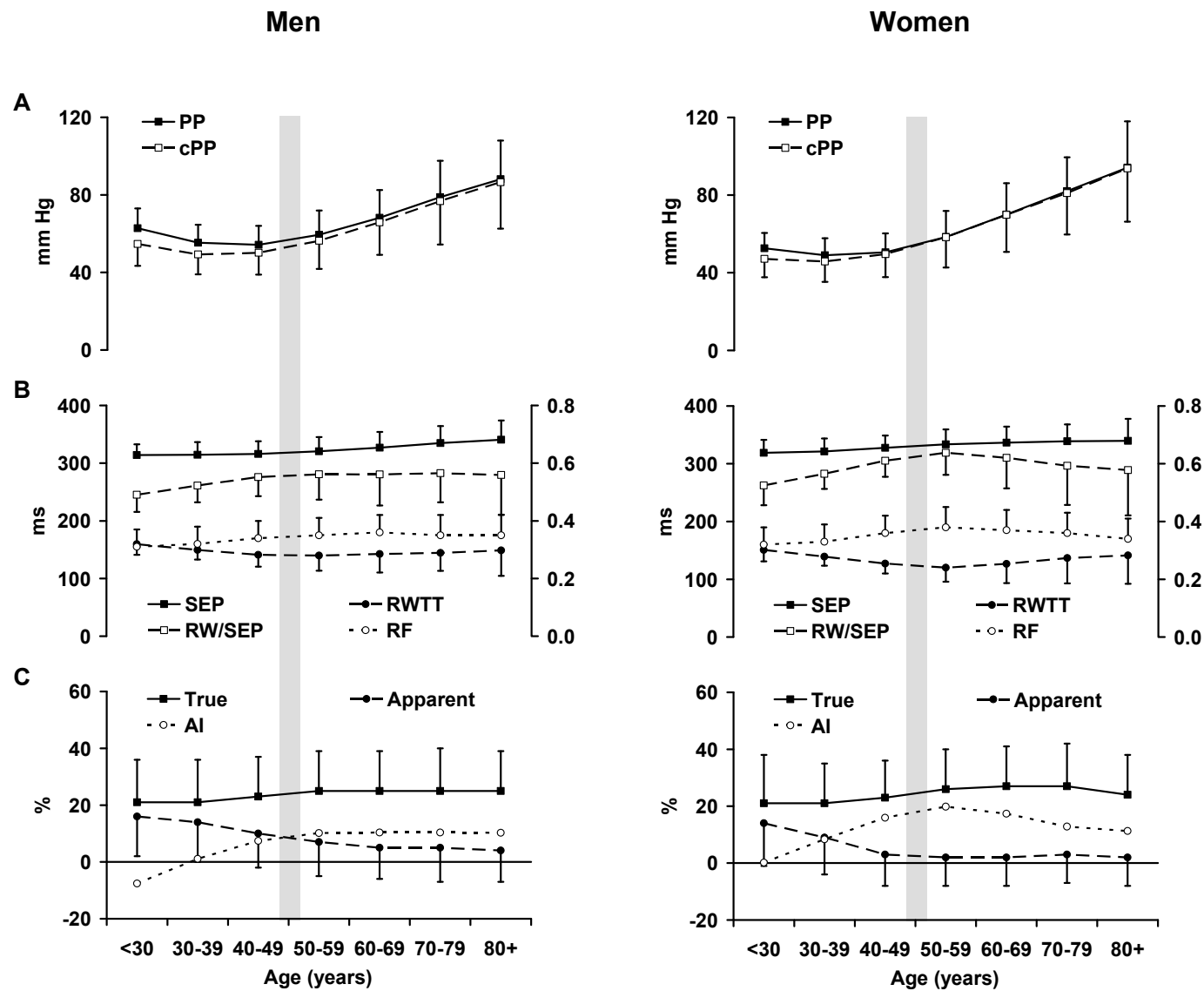
Supplemental Figure S2.



Supplemental Figure S3.



Supplemental Figure S4.



Supplemental References

1. Kelly R, Fitchett D. Noninvasive determination of aortic input impedance and external left ventricular power output: a validation and repeatability study of a new technique. *J Am Coll Cardiol*. 1992;20:952-963.
2. Mitchell GF, Izzo JL, Jr., Lacourciere Y, Ouellet JP, Neutel J, Qian C, Kerwin LJ, Block AJ, Pfeffer MA. Omapatrilat reduces pulse pressure and proximal aortic stiffness in patients with systolic hypertension: results of the conduit hemodynamics of omapatrilat international research study. *Circulation*. 2002;105:2955-2961.
3. Murgu JP, Westerhof N, Giolma JP, Altobelli SA. Aortic input impedance in normal man: relationship to pressure wave forms. *Circulation*. 1980;62:105-116.
4. Mitchell GF, Tardif JC, Arnold JM, Marchiori G, O'Brien TX, Dunlap ME, Pfeffer MA. Pulsatile hemodynamics in congestive heart failure. *Hypertension*. 2001;38:1433-1439.
5. Westerhof N, Sipkema P, Van Den Bos GC, Elzinga G. Forward and backward waves in the arterial system. *Cardiovasc Res*. 1972;6:648-656.
6. Liu Z, Brin KP, Yin FC. Estimation of total arterial compliance: an improved method and evaluation of current methods. *Am J Physiol*. 1986;251:H588-H600.